THE JOURNAL OF PHYSICAL CHEMISTRY Letters

Letter

Cite This: J. Phys. Chem. Lett. 2019, 10, 748−753

pubs.acs.org/JPCL

Lighting Up the Invisible Twisted Intramolecular Charge Transfer State by High Pressure

Hui Li,[†] Jianhui Han,[†] Huifang Zhao,[†] Xiaochun Liu,[†] Yi Luo,[‡] Ying Shi,*[,†] Cailong Liu,*[,†] Mingxing Jin,[†] and Dajun Ding*[,†]

[†]Institute of Atomic and Molecular Physics, Jilin University, Changchun 130012, China

[‡]Hefei National Laboratory for Physical Sciences at the Microscale, University of Science and Technology of China, Hefei, Anhui 230026, China

Supporting Information

ABSTRACT: The twisted intramolecular charge transfer (TICT) state plays an important role in determining the performance of optoelectronic devices. However, for some nonfluorescent TICT molecules, the "invisible" TICT state could only be visualized by modifying the molecular structure. Here, we introduce a new facile pressure-induced approach to light up the TICT state through the use of a pressure-related liquid−solid phase transition of the surrounding solvent. Combining ultrafast spectroscopy and quantum chemical calculations, it reveals that the "invisible" TICT state can emit fluorescence when the rotation of a donor group is restricted by the frozen acetonitrile solution. Furthermore, the TICT process can even be effectively regulated by the external pressure. Our study offers a unique strategy to achieve dual fluorescence behavior in charge transfer molecules and is of significance for optoelectronic and biomedical applications.

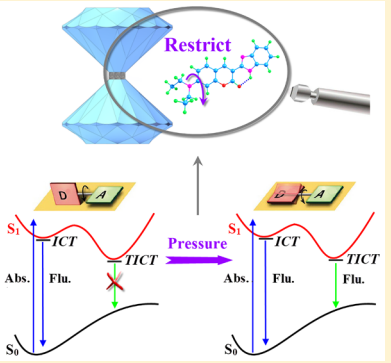

Twisted intramolecular charge transfer (TICT) is an elementary and important photophysical and photochemical process.[1−5] The TICT process is accompanied by rotational relaxation around a bond connecting the intramolecular electron donor and acceptor groups. TICT state is an emission state in some molecules like *p*-*N*,*N*-dimethylaminobenzonitrile (DMABN), which was proposed by Grabowski to explain the anomalous emission.[6] Especially, the TICT state also exhibits nonfluorescent and low-fluorescence phenomena.[7−9] For the nonfluorescent TICT molecules, effectively lighting up the invisible TICT state is crucial for developing a variety of promising applications, such as fluorescing probes, optical sensors, and solar energy harvesting devices.[10−16] Previous works on visualizing the TICT state have involved molecular structure modifications, such as altering the substituted position or rigidifying the torsional group.[17,18] However, on the basis of the intrinsic molecular configuration, the ability to tune the TICT state from invisible to visible has yet to be realized. Understanding the mechanism for how to achieve *in situ* regulation of TICT fluorescence can further provide a critical step toward promising optoelectronic and biomedical applications.

We introduce a new and facile method for lighting up the TICT state using *in situ* high-pressure technology. An environmentally sensitive molecular system is placed in a solvent that can undergoes pressure-induced liquid−solid phase transition to restrict the rotation of the molecular groups. In conjunction with *in situ* high-pressure steady fluorescence spectroscopy, we have been able to observe fluorescence from the TICT state. To the best of our knowledge, this unique feature has never been achieved before.

The chosen environmentally sensitive molecule in this work is coumarin 7 (C7). C7 contains a rotating 7-*N*,*N*-diethylamino (7-NEt_2) group and participates in a nonfluorescent TICT process.[19,20] Figure 1 schematically illustrates the photophysical picture describing the relaxation mechanism in such molecular systems. Upon photoexcitation to the first excited state, C7 initially forms an intramolecular charge transfer (ICT) state. Thereafter, with the rotational relaxation between the donor and acceptor groups, C7 produces a twisted conformation and forms the TICT state. The ICT state is usually associated with fluorescence while the TICT state is nonfluorescent. The C7 molecule was chosen as the model system for two reasons: On the one hand, the formation of an intramolecular hydrogen bond in the C7 molecule makes the torsional behaviors occur only on the single bond connecting the 7-NEt_2 group and other parts. This structure character would be helpful to regulate this TICT process individually. On the other hand, the C7 molecule has been demonstrated to be a good probe for environmentally sensitive tracking. This is highly beneficial to the observation of the dynamic TICT process under high pressure.

Figure 2 shows the steady-state fluorescence spectra of the C7 dye in acetonitrile (ACN) solvent under increasing

Received: January 5, 2019
Accepted: January 31, 2019
Published: January 31, 2019

DOI: 10.1021/acs.jpclett.9b00026
J. Phys. Chem. Lett. 2019, 10, 748−753

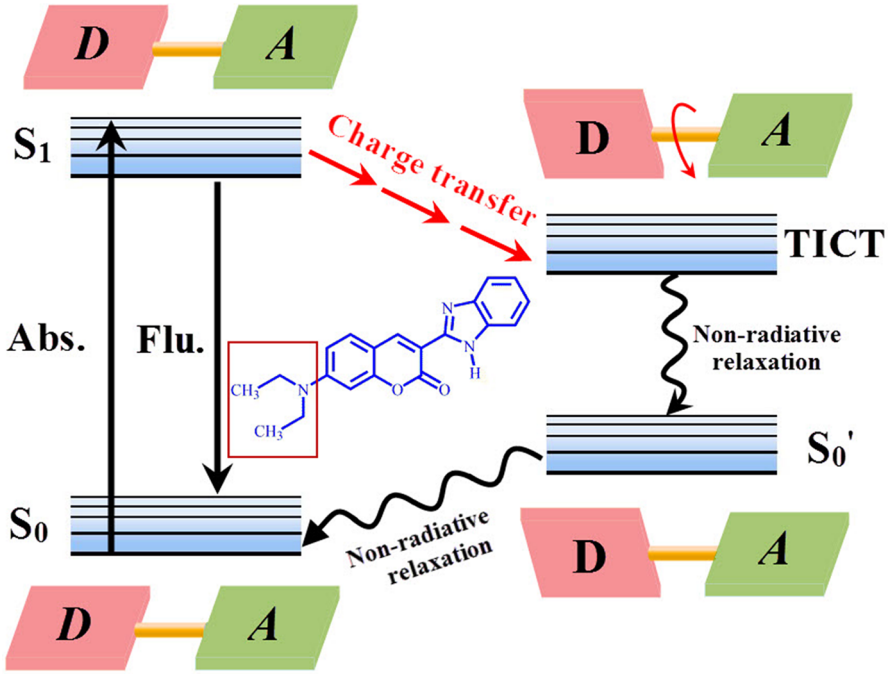

Figure 1. Schematic illustration of the relaxation mechanism in the C7 molecule. D represents the donor group, and A represents the acceptor group.

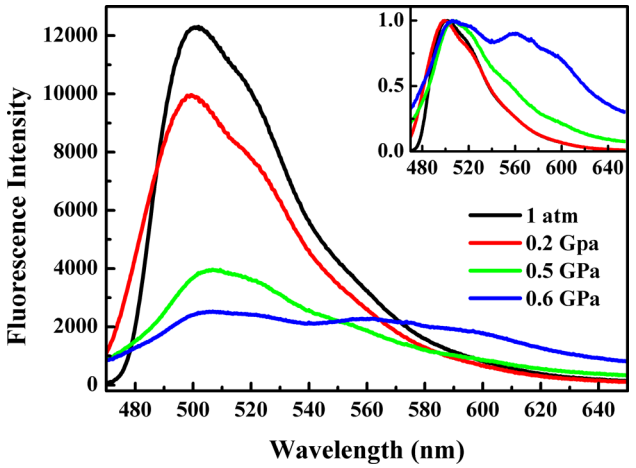

Figure 2. Measured fluorescence spectra of the C7 molecule at different pressures from 1 atm to 0.6 GPa. The inset corresponds to the normalized results of fluorescence spectra.

pressure. It can be noted clearly that the spectrum at 1 atm exhibited a single-peak emission centered at 501.8 nm. With increasing pressure, the intensity of the emission dropped significantly. A closer look at the corresponding normalized results (inset of Figure 2) reveals that the emission peak shifts to the red side and the half-width of the band becomes much broader. It must be noted that ACN was found to be frozen at a pressure of 0.5 GPa during compression, as Olejniczak also reports.[21] Interestingly, after elevating the pressure to 0.6 GPa, except for the prime fluorescence peak at 506.8 nm, a new fluorescence peak at 560.1 nm appeared. We speculate that the single fluorescence at 1 atm should come from the ICT state, while the new peak is derived from pressure-induced fluorescence of the TICT state.

To gain insight into the dynamic evolution of the C7 molecule in the liquid and solid phase of ACN, *in situ* high-pressure TA spectroscopy was employed. Global fitting was used to analyze the relaxation dynamics of the excited-state C7 molecule with sets of kinetic curves simultaneously. Regardless of the ACN phase (liquid or solid), the relaxation process could be satisfied with three exponentials of lifetimes τ_1, τ_2, and τ_3.

$$A(t) = \sum_{i=1} a_i \exp\left(-\frac{t}{\tau_i}\right) \quad (1)$$

a_i and τ_i are amplitudes and the characteristic time associated with each component, respectively. Combining this study with that of Pal et al.,[19] the first process (τ_1) can be attributed to the ICT process, and the second process (τ_2) should be derived from the TICT process. The slower τ_3 lifetime of only a few nanoseconds should be assigned to the fluorescence lifetime. Figure 3 shows the evaluation for the best-fit curves using a global analysis. During the compression process in liquid-phase ACN, we observed that the time constants of τ_1 and τ_2 were slowed down remarkably. At the liquid−solid phase transformation pressure for ACN (0.5 GPa), the values of τ_1 and τ_2 increased from 0.3 and 64.5 ps at 1 atm to 1.9 and 131.8 ps, respectively. In the solid phase of ACN under further increased pressure, the two processes were facilitated and finally reached 1.1 ps (τ_1) and 90.4 ps (τ_2). Nevertheless, unlike τ_1 and τ_2 processes, we found that the fitted slowest decay process (τ_3) continued to slow down during the process of compression.

To understand the novel phenomenon better, comprehensive quantum chemistry calculations were investigated. We shows the optimized geometry for C7 in ACN (Supporting Information, Figure S1) for the first excited S_1 state (ICT state) and a near-perpendicular twisted conformer in the S_1' state (TICT state). At 1 atm, the calculated dihedral angles D_1 (C4N1C2C1) were found to be 2 and 92° in the ICT and TICT state, respectively. The fluorescence peaks of the ICT and TICT states were also calculated, and the fluorescence

DOI: 10.1021/acs.jpclett.9b00026
J. Phys. Chem. Lett. 2019, 10, 748−753

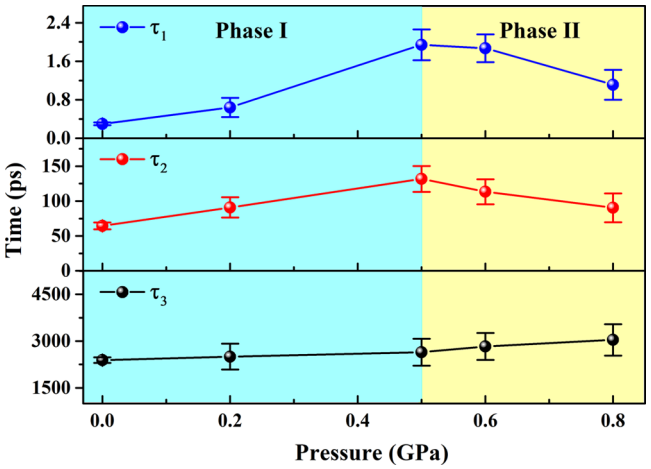

Figure 3. Fitted transient absorption kinetic lifetimes of the C7 molecule by global analysis at different pressures from 1 atm to 0.6 GPa. Blue represents the liquid phase of ACN solvent, and yellow represents the solid phase.

peak from ICT was calculated to be 504.2 nm, closely resembling the 501.8 nm measured experimentally. The fluorescence of the TICT state was calculated at 702.1 nm, which was not observed in the experiment. Thus, the calculations predict that the only observable fluorescence at 1 atm should originate from the ICT state, while the TICT state does not fluoresce.

The decouple effect between the electronic donor and the acceptor in a twisted structure is a main factor for the nonfluorescent TICT state phenomenon.[22] Figure 4 plots the relevant frontier molecular orbitals (MOs) of the S_1 and S_1' states. A remarkable charge transfer signature of the ICT and TICT processes lying along the twisted coordinate of the 7-NEt_2 group can be observed. Importantly, we found that the strong coupling effect between the HOMO and LUMO happens in the ICT molecule, indicating that fluorescence from the ICT state is allowed. However, the corresponding overlap at the twisted structure of the TICT process is nearly zero. Thus, the weak coupling of charge density forbids TICT emission in the excited C7 molecule. We scanned the variation of S_0 and S_1 state energies as a function of the twist dihedral angle D_1, depicted in Figure S2. On the basis of the different twist configurations of C7 in the S_1 state at 1 atm, the coupling effect between the HOMO and LUMO was investigated further. As Figure 4 displays (typically at torsion angles of 30, 50, and 70°), strong coupling effects between the HOMO and LUMO are exhibited, except at the $D_1 = 92°$ twisted structure.[9] This means that as long as the 7-NEt_2 group is not rotated to $D_1 = 92°$ fluorescence will be allowed.

We can form a convincing explanation for the two observed emission phenomena when C7 is compressed to 0.6 GPa. In the ACN liquid phase, solvent viscosity is a key factor affecting rotation of the 7-NEt_2 group. According to the relationship proposed by Ducoulombier et al[23]

$$\eta = \exp(aP^2 + bP + c) \quad (2)$$

a, b, and c are constants, and the solvent viscosity (η) can be increased by elevating the pressure (P). Combining with the Stokes−Einstein−Debye theory,[24,25] the increasing viscosity of the solvent can slow down the rotational rate of the 7-NEt_2 group, giving a reasonable explanation for the slower TICT

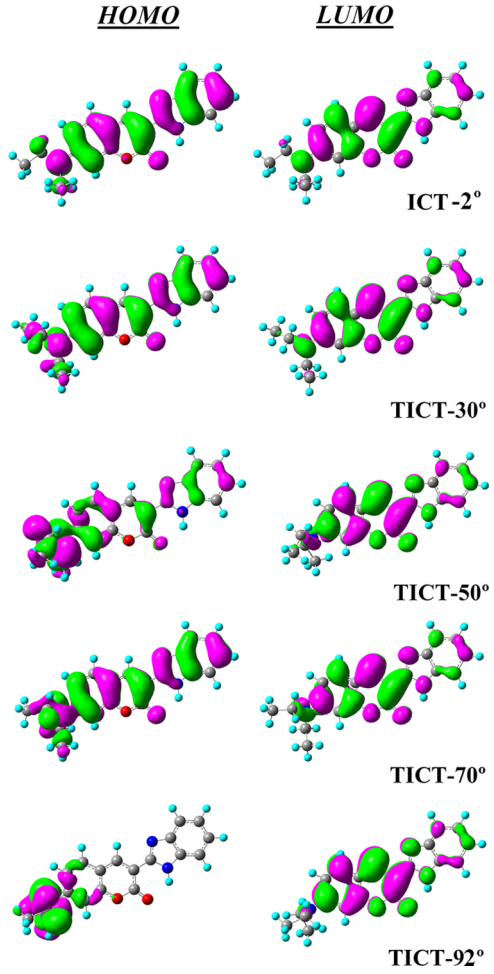

Figure 4. Plotted frontier molecular orbitals in the S_1 state for C7 dye at torsion angles of 2, 30, 50, 70, and 92°.

rate with increasing pressure in our TA experiment. However, viscosity can only slow down the rotational rate of the 7-NEt_2 group; it cannot restrict torsion of the 7-NEt_2 group. This was proved by the steady-state fluorescence experiment of C7 in a high-viscosity solvent at 1 atm (Supporting Information, Figure S3). Therefore, the excited C7 will fully relax to the most stable nonfluorescing TICT configuration. However, when the environment around the C7 molecules change from the liquid to solid phase (0.6 GPa), the lattice structure of crystallized ACN becomes the essential effect,[26] resulting in acceleration of the 7-NEt_2 rotation rate with increasing pressure in TA experiments. According to the reports of Li et al.,[17] as the molecular order increases, the free intramolecular configuration twist of the 7-NEt_2 group will become more restricted. The full relaxing of C7 to the most stable nonfluorescent TICT configuration is significantly hindered. As Figure 4 describes, at 0.6 GPa, the twist dihedral angle of the 7-NEt_2 group is fixed at an intermediate value ($D_1 < 92°$), which induces coupling of charge density between the electronic donor and acceptor to significantly increase. Therefore, a "visible" TICT state with fluorescence emission could be formed.

As we know, the viscosity of solvent can be increased under high pressure, which will suppress the TICT process and enhance the emission of the ICT state. However, with increasing pressure, we found that the fluorescent intensity of the ICT state decreases (Figure 2). It cannot be ignored that

DOI: 10.1021/acs.jpclett.9b00026
J. Phys. Chem. Lett. 2019, 10, 748−753

the emission intensity of the ICT state is closely related to not only the viscosity but also the polarity of solvent. On the basis of the report of Srinivasan, with increasing pressure, the dielectric constant as an index of polarity of acetonitrile solvent also increases.[27] Furthermore, according to the previous studies of Pal et al. on a series of coumarin molecules, they reported that as the polarity increases the emission intensity of the ICT state can be suppressed, while the TICT state can be promoted.[28] We further measured the fluorescence spectra of C7 at 1 atm in different solvents with similar viscosity but different polarity, which further showed that the emission intensity of the ICT state is dependent on the solvent polarity (Supporting Information, Table S1 and Figure S4). Thus, high pressure induces enhancement of the polarity of ACN solvent, resulting in a decrease of the emission intensity of the ICT state.

In summary, a novel single-fluorescence phenomenon of the C7 molecule in ACN resulted in two emissions at a pressure of 0.6 GPa. Combined with a DFT/TDDFT theoretical study, we demonstrated that one of the fluorescence peaks was derived from the ICT state of the C7 molecule, while the new peak was derived from a newly formed TICT state with the twist dihedral angle $D_1 < 92°$. Pressure-induced solidification of the ACN solvent increased the molecular ordering of C7 and caused the intramolecular twist configuration of the 7-NEt_2 group to be more restricted. Thus, forbidden fluorescence from the TICT state was turned into permitted fluorescence. Furthermore, *in situ* high-pressure ultrafast spectroscopy revealed that the torsion rate of the 7-NEt_2 group can be regulated effectively by pressure-induced liquid−solid phase transformation of the solvent. Our study confirmed that high pressure can light up the invisible TICT state of C7 successfully. This facile, yet robust, approach is expected to provide a new strategy for designing more versatile photoluminescent materials.

EXPERIMENTAL METHODS

C7 was purchased from Sigma−Aldrich and was used without further purification. Acetonitrile (superdry, spectroscopy grade) was obtained from J&K (China). ACN was chosen as the pressure-transmitting medium due to the low pressure needed for a liquid−solid phase transition.[21] C7 was dissolved in ACN to a concentration of 1×10^{-3} M. C7 dye is known to exist in a monomeric form when dissolved in ACN.[29]

A tungsten lamp was used as the light source for steady absorption spectroscopy. The light was dispersed with an optical fiber spectrometer, and the output spectra were recorded on a computer. For the fluorescence spectra measurement, a 400 nm semiconductor laser was used to excite the sample. The output power was 150 mw. Interference and color filters were used to exclude the extraneous radiation in the emission path. A high-resolution fiber optic spectrometer (HR4000, Ocean Optical) was used to collect all of the measured signals.

The details for the femtosecond transient absorption apparatus are discussed elsewhere.[30−34] The femtosecond laser (Coherent Libra, U.S.) source was an all-in-one ultrafast oscillator and a regenerative amplifier. The laser system provided 4 mJ pulses with a repetition rate of 1000 Hz. The output wavelength was 800 nm with a duration of 50 fs. The excitation wavelength was 400 nm, and the energy per pulse at the sample was approximately 4 μJ. The pump and probe laser beams were incident on the diamond anvil cell (DAC) at a small angle ($\theta \leq 5°$).

The DAC was used to generate high pressure. The pressure inside of the sample compartment was calibrated by the R_1 fluorescence shift of the ruby chips.[35,36] ACN solvent was used as the pressure-transmitting medium. All of the measurements were performed at room temperature (295 K).

COMPUTATIONAL METHODOLOGY

Molecular geometries in the ground and low-lying first singlet excited states at 1 atm were fully optimized using density functional theory (DFT) and the time-dependent density functional theory (TD-DFT).[37−41] Compared to other functionals employed (Supporting Information, Table S2), using the B3LYP functional[42] (Becke's three parameter exchange functional (B3) with the nonlocal correlation functional by Lee, Yang, and Parr (LYP)) produced calculated fluorescence peak values that were in good agreement with the experimental peak values. Therefore, B3LYP was selected for this study. The triple-ζ valence quality basis with one set of polarization functions (TZVP) was chosen throughout,[43] and the solvent effects were included using the integral equation formalism (IEF) version of the polarizable continuum model (PCM).[44−46] The Gaussian program was used to perform all of the quantum chemical calculations.[47]

ASSOCIATED CONTENT

Supporting Information

The Supporting Information is available free of charge on the ACS Publications website at DOI: 10.1021/acs.jpclett.9b00026.

Optimized structures, scanned potential energy profiles, measured fluorescence spectra, summarized viscosity, polarity, and dielectric constant, and calculated excited energy, corresponding oscillator strengths and fluorescence peaks, and orbital transitions and contributions (PDF)

AUTHOR INFORMATION

Corresponding Authors

*E-mail: shi_ying@jlu.edu.cn (Y.S.).
*E-mail: cailong_liu@jlu.edu.cn (C.L.).
*E-mail: dajund@jlu.edu.cn (D.D.).

ORCID

Ying Shi: 0000-0002-6240-8795
Cailong Liu: 0000-0003-0702-7225

Notes

The authors declare no competing financial interest.

ACKNOWLEDGMENTS

This work was supported by the National Basic Research Program of China (973 Program) (2013CB922204) and the National Natural Science Foundation of China (No. 11874180).

REFERENCES

(1) Wiedbrauk, S.; Maerz, B.; Samoylova, E.; Mayer, P.; Zinth, W.; Dube, H. Ingredients to TICT Formation in Donor Substituted Hemithioindigo. *J. Phys. Chem. Lett.* **2017**, *8*, 1585−1592.

(2) Teran, N. B.; He, G. S.; Baev, A.; Shi, Y.; Swihart, M. T.; Prasad, P. N.; Marks, T. J.; Reynolds, J. R. Twisted Thiophene-Based Chromophores with Enhanced Intramolecular Charge Transfer for

DOI: 10.1021/acs.jpclett.9b00026
J. Phys. Chem. Lett. 2019, 10, 748−753

Cooperative Amplification of Third-Order Optical Nonlinearity. *J. Am. Chem. Soc.* **2016**, *138*, 6975−6984.
(3) Olsen, S.; Smith, S. C. Radiationless Decay of Red Fluorescent Protein Chromophore Models Via Twisted Intramolecular Charge-Transfer States. *J. Am. Chem. Soc.* **2007**, *129*, 2054−2065.
(4) Cha, W. Y.; Lim, J. M.; Park, K. H.; Kitano, M.; Osuka, A.; Kim, D. Two Modes of Photoinduced Twisted Intramotecular Charge Transfer in Meso-Arylaminated Subporphyrins. *Chem. Commun.* **2014**, *50*, 8491−8494.
(5) Cong, L.; Yin, H.; Shi, Y.; Jin, M. X.; Ding, D. J. Different Mechanisms of Ultrafast Excited State Deactivation of Coumarin 500 in Dioxane and Methanol Solvents: Experimental and Theoretical Study. *RSC Adv.* **2015**, *5*, 1205−1212.
(6) Rotkiewicz, K.; Grellmann, K. H.; Grabowski, Z. R. Reinterpretation of the anomalous fluorescense of p-N,N-dimethylamino-benzonitrile. *Chem. Phys. Lett.* **1973**, *19*, 315−318.
(7) Rafiq, S.; Yadav, R.; Sen, P. Femtosecond Excited-State Dynamics of 4-Nitrophenyl Pyrrolidinemethanol: Evidence of Twisted Intramolecular Charge Transfer and Intersystem Crossing Involving the Nitro Group. *J. Phys. Chem. A* **2011**, *115*, 8335−8343.
(8) Szakács, Z.; Rousseva, S.; Bojtár, M.; Hessz, D.; Bitter, I.; Kállay, M.; Hilbers, M.; Zhang, H.; Kubinyi, M. Experimental evidence of TICT state in 4-piperidinyl-1,8-naphthalimide − a kinetic and mechanistic study. *Phys. Chem. Chem. Phys.* **2018**, *20*, 10155−10164.
(9) Ghosh, R.; Palit, D. K. Effect of donor−acceptor coupling on TICT dynamics in the excited states of two dimethylamine substituted chalcones. *J. Phys. Chem. A* **2015**, *119*, 11128−11137.
(10) Chen, B.; Sun, X.; Li, X.; Ågren, H.; Xie, Y. TICT based fluorescence "turn-on" hydrazine probes. *Sens. Actuators, B* **2014**, *199*, 93−100.
(11) Ghosh, S.; Roscioli, J. D.; Bishop, M. M.; Gurchiek, J. K.; LaFountain, A. M.; Frank, H. A.; Beck, W. F. Torsional Dynamics and Intramolecular Charge Transfer in the S_2 ($1^1B_U^+$) Excited State of Peridinin: A Mechanism for Enhanced Mid Visible Light Harvesting. *J. Phys. Chem. Lett.* **2016**, *7*, 3621−3626.
(12) Sasaki, S.; Drummen, G. P. C.; Konishi, G. Recent advances in twisted intramolecular charge transfer (TICT) fluorescence and related phenomena in materials chemistry. *J. Mater. Chem. C* **2016**, *4*, 2731−2743.
(13) Zhao, G. J.; Han, K. L. pH-Controlled twisted intramolecular charge transfer (TICT) excited state via changing the charge transfer direction. *Phys. Chem. Chem. Phys.* **2010**, *12*, 8914−8918.
(14) Wiedbrauk, S.; et al. Twisted Hemithioindigo Photoswitches: Solvent Polarity Determines the Type of Light-Induced Rotations. *J. Am. Chem. Soc.* **2016**, *138*, 12219−12227.
(15) Lou, A. J.-T.; et al. Unprecedented Large Hyperpolarizability of Twisted Chromophores in Polar Media. *J. Am. Chem. Soc.* **2018**, *140*, 8746−8755.
(16) Chábera, P.; et al. A low-spin Fe(iii) complex with 100-ps ligand-to-metal charge transfer photoluminescence. *Nature* **2017**, *543*, 695.
(17) Li, J.; Qian, Y.; Xie, L.; Yi, Y.; Li, W.; Huang, W. From dark TICT State to emissive quasi-TICT State: The AIE mechanism of N-(3-(benzo[d]oxazol-2-yl)phenyl)-4-tert-butylbenzamide. *J. Phys. Chem. C* **2015**, *119*, 2133−2141.
(18) Liu, X.; Qiao, Q.; Tian, W.; Liu, W.; Chen, J.; Lang, M. J.; Xu, Z. Aziridinyl fluorophores demonstrate bright fluorescence and superior photostability by effectively inhibiting twisted intramolecular charge transfer. *J. Am. Chem. Soc.* **2016**, *138*, 6960−6963.
(19) Satpati, A.; Senthilkumar, S.; Kumbhakar, M.; Nath, S.; Maity, D. K.; Pal, H. Investigations of the solvent polarity effect on the photophysical properties of coumarin-7 Dye. *Photochem. Photobiol.* **2005**, *81*, 270−278.
(20) Chandrasekaran, S.; Sameena, Y.; Enoch, I. Modulation of the interaction of Coumarin 7 with DNA by beta-cyclodextrin. *J. Inclusion Phenom. Macrocyclic Chem.* **2015**, *81*, 225−236.
(21) Olejniczak, A.; Katrusiak, A. Supramolecular reaction between pressure-frozen acetonitrile phases alpha and beta. *J. Phys. Chem. B* **2008**, *112*, 7183−7190.
(22) Soujanya, T.; Fessenden, R. W.; Samanta, A. Role of nonfluorescent twisted intramolecular charge transfer state on the photophysical behavior of aminophthalimide Dyes. *J. Phys. Chem.* **1996**, *100*, 3507−3512.
(23) Ducoulombier, D.; Zhou, H.; Boned, C.; Peyrelasse, J.; Saint-Guirons, H.; Xans, P. Pressure (1−1000 bar) and temperature (20−100. degree. C) dependence of the viscosity of liquid hydrocarbons. *J. Phys. Chem.* **1986**, *90*, 1692−1700.
(24) Barooah, N.; Mohanty, J.; Pal, H.; Bhasikuttan, A. C. Non-covalent interactions of coumarin dyes with cucurbit[7]uril macrocycle: modulation of ICT to TICT state conversion. *Org. Biomol. Chem.* **2012**, *10*, 5055−5062.
(25) Singh, A. K.; Ramakrishna, G.; Ghosh, H. N.; Palit, D. K. Photophysics and ultrafast relaxation dynamics of the excited states of dimethylaminobenzophenone. *J. Phys. Chem. A* **2004**, *108*, 2583−2597.
(26) Wang, Z. W.; Schliehe, C.; Wang, t.; Nagaoka, Y.; Cao, Y. C.; Bassett, W. A.; Wu, H.; Fan, H.; Weller, H. Deviatoric Stress Driven Formation of Large Single-Crystal PbS Nanosheet from Nanoparticles and in Situ Monitoring of Oriented Attachment. *J. Am. Chem. Soc.* **2011**, *133*, 14484−14487.
(27) Srinivasan, K. R.; Kay, R. L. The pressure dependence of the dielectric constant and density of acetonitrile at three temperatures. *J. Solution Chem.* **1977**, *6*, 357−367.
(28) Nad, S.; Kumbhakar, M.; Pal, H. Photophysical properties of coumarin-152 and coumarin-481 dyes: unusual behavior in nonpolar and in higher polarity solvents. *J. Phys. Chem. A* **2003**, *107*, 4808−4816.
(29) Verma, P.; Pal, H. Intriguing H-aggregate and H-dimer formation of coumarin-481 dye in aqueous solution as evidenced from photophysical studies. *J. Phys. Chem. A* **2012**, *116*, 4473−4484.
(30) Wu, B.; Hu, J.; Cui, P.; Jiang, L.; Chen, Z.; Zhang, Q.; Luo, Y.; Wang, C. Visible-light photoexcited electron dynamics of scandium endohedral metallofullerenes: The cage symmetry and substituent effects. *J. Am. Chem. Soc.* **2015**, *137*, 8769−8774.
(31) Liu, X. C.; Han, J. H.; Zhao, H. F.; Yan, H. C.; Shi, Y.; Jin, M. X.; Liu, C. L.; Ding, D. J. Pressure dependence of excited-state charge-carrier dynamics in organolead tribromide perovskites. *Appl. Phys. Lett.* **2018**, *112*, 191903.
(32) Yin, H.; Li, H.; Xia, G.; Ruan, C.; Shi, Y.; Wang, H.; Jin, M. X.; Ding, D. A novel non-fluorescent excited state intramolecular proton transfer phenomenon induced by intramolecular hydrogen bonds: an experimental and theoretical investigation. *Sci. Rep.* **2016**, *6*, 19774.
(33) Hu, J.; Zhang, Q.; Luo, Y. Retrieving the rate of reverse intersystem crossing from ultrafast spectroscopy. *J. Phys. Chem. Lett.* **2016**, *7*, 3908−3912.
(34) Alberding, B. G.; Chisholm, M. H.; Gallucci, J. C.; Ghosh, Y.; Gustafson, T. L. Electron delocalization in the S1 and T1 metal-to-ligand charge transfer states of trans-substituted metal quadruply bonded complexes. *Proc. Natl. Acad. Sci. U. S. A.* **2011**, *108*, 8152−8156.
(35) Wang, T.; Li, R.; Quan, Z.; Loc, W. S.; Bassett, W. A.; Xu, H.; Cao, Y.; Fang, J.; Wang, Z. Pressure processing of nanocube assemblies toward harvesting of a metastable PbS phase. *Adv. Mater.* **2015**, *27*, 4544−4549.
(36) Liu, C.; Mafety, A.; Queyroux, J. A.; Wilson, C. W.; Zhang, H.; Beneut, K.; Finocchi, F.; et al. Topologically frustrated ionisation in a water-ammonia ice mixture. *Nat. Commun.* **2017**, *8*, 1065.
(37) Fang, Y. R.; Sun, M. T. Nanoplasmonic waveguides: towards applications in integrated nanophotonic circuits. *Light: Sci. Appl.* **2015**, *4*, No. e294.
(38) Sun, M.; Fang, Y.; Yang, Z.; Xu, H. Chemical and electromagnetic mechanisms of tip-enhanced Raman scattering. *Phys. Chem. Chem. Phys.* **2009**, *11*, 9412−9419.
(39) Vahtras, O.; Almlöf, J.; Feyereisen, M. W. Integral approximations for LCAO-SCF calculations. *Chem. Phys. Lett.* **1993**, *213*, 514−518.
(40) Zhou, P.; Liu, J.; Yang, S.; Chen, J.; Han, K.; He, G. The invalidity of the photo-induced electron transfer mechanism for

DOI: 10.1021/acs.jpclett.9b00026
J. Phys. Chem. Lett. 2019, 10, 748−753

fluorescein derivatives. *Phys. Chem. Chem. Phys.* **2012**, *14*, 15191−15198.
(41) Zhang, Y.; Hua, W.; Bennett, K.; Mukamel, S. *Nonlinear spectroscopy of core and valence excitations using short X-Ray pulses: simulation challenges. Density-functional methods for excited states*; Ferré, N., Filatov, M., Huix-Rotllant, M., Eds.; Springer International Publishing: Cham, 2016; pp 273−345.
(42) Song, P.; Li, Y.; Ma, F.; Pullerits, T.; Sun, M. External electric field-dependent photoinduced charge transfer in a donor−acceptor system for an organic solar cell. *J. Phys. Chem. C* **2013**, *117*, 15879−15889.
(43) Deglmann, P.; Furche, F. Efficient characterization of stationary points on potential energy surfaces. *J. Chem. Phys.* **2002**, *117*, 9535−9538.
(44) Cammi, R.; Tomasi, J. Remarks on the use of the apparent surface charges (ASC) methods in solvation problems: Iterative versus matrix-inversion procedures and the renormalization of the apparent charges. *J. Comput. Chem.* **1995**, *16*, 1449−1458.
(45) Cancès, E.; Mennucci, B.; Tomasi, J. A new integral equation formalism for the polarizable continuum model: Theoretical background and applications to isotropic and anisotropic dielectrics. *J. Chem. Phys.* **1997**, *107*, 3032−3041.
(46) Mennucci, B.; Cancès, E.; Tomasi, J. Evaluation of solvent effects in isotropic and anisotropic dielectrics and in ionic solutions with a unified integral equation method: Theoretical bases, computational implementation, and numerical applications. *J. Phys. Chem. B* **1997**, *101*, 10506−10517.
(47) Frisch, M. J.; et al. *Gaussian 09*; Gaussian, Inc.: Wallingford, CT, 2009.

DOI: 10.1021/acs.jpclett.9b00026
J. Phys. Chem. Lett. 2019, 10, 748−753